A Machine Learning Approach to Modeling and Identification of Automotive Three-Way Catalytic Converters

Luigi Glielmo, *Member, IEEE*, Michele Milano, and Stefania Santini

Abstract—The working of three-way catalytic converters (TWC's) is based on chemical reactions whose rates are nonlinear functions of temperature and reactant concentrations all along the device. Unfortunately, the choice of suitable expressions and the *tuning* of their parameters is particularly difficult in dynamic conditions. In this paper, we introduce a hybrid modeling technique which allows us to preserve the most important features of an accurate distributed parameter TWC model, while it circumvents both the structural and the parameter uncertainties of "classical" reaction kinetics models, and saves computational time. In particular, we compute the rates within the TWC dynamic model by a neural network which, thus, becomes a static nonlinear component of a larger dynamic system. A purposely designed genetic algorithm, in conjunction with a fast *ad hoc* partial differential equation integration procedure, allows us to train the neural network, embedded in the whole model structure, using currently available measurement data and without computing gradient information.

Index Terms—Genetic algorithms, neural network applications, parameter estimation, partial differential equations, road vehicles.

I. INTRODUCTION AND MOTIVATIONS

TO PREVENT the emission of harmful components by automotive gasoline engine, vehicles are equipped with a three-way catalytic converter (TWC) which is located in the exhaust pipe (see Fig. 1). Usually, modern converters are of the monolithic type, a block of ceramic material with thousands of parallel channels (tubular reactor) maximizing the exposed surface area; exhaust gas flows through the reticular structure of this honeycomb ceramic block and is adsorbed by the catalytic surface where it reacts. As is well known, the rate of chemical reactions can be affected by the presence of the so-called catalysts; catalysts are agents that reduce the activation energy of the reaction of interest, generally without being transformed throughout the reactive chain. Most of the catalysts used in gas-phase reactions are noble metals or metal oxides. In the emission treatment system the ceramic block, mounted in a stainless steel container,

L. Glielmo and S. Santini are with the Group of Research on Automotive Control Engineering, Dipartimento di Informatica e Sistemistica, Universita di Napoli Federico II, Naples, Italy (e-mail: glielmo@unina.it; stsantin@unina.it).

M. Milano is with the Institue of Fluid Dynamics, Swiss Federal Institute of Technology, CH-8092 Zurich, Switzerland (e-mail: milano@ifd.mavt.ethz.ch).
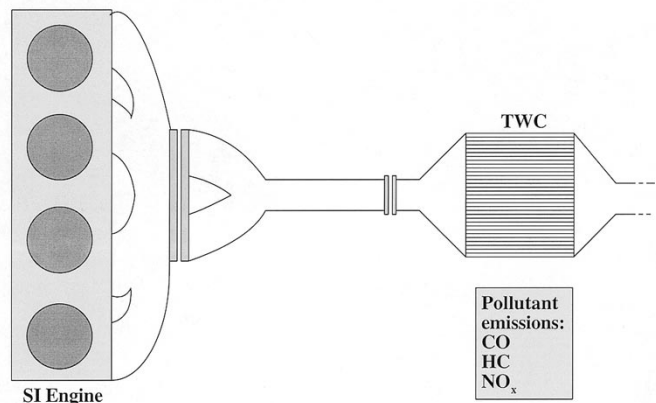
Fig. 1.   Emission treatment system and major pollutant components.

is usually covered by a thin coating of platinum, rhodium, or palladium.

The TWC removes carbon monoxide, oxides of nitrogen, and hydrocarbons. To allow the catalyzed reactions to proceed simultaneously, reaching high conversion efficiencies (more than 95%), the TWC has to be sufficiently warmed up (above 600 K) and the air–fuel mixture in the combustion chamber has to be regulated around the stoichiometric point by a control system. In particular, the TWC is said to *light off* when hydrocarbons conversion efficiency reaches 50%. Unfortunately, in many conditions of practical interest, such as cold start, warm-up, transient acceleration, and transient fuel cutoff during decelerations, the TWC works out of the required temperature and/or stoichiometric ranges.

In view of this and future stricter legislation on engine exhaust gases, the so-called ultra low vehicle emissions (ULVE, for the year 2000 and beyond), the optimization of the TWC dynamic behavior will become critical. An important task toward the online optimization of engine fueling strategies is to predict the transient TWC emissions for any driving condition with a reasonable computational load. In the literature, one can find many detailed physics- and chemistry-based models (see, for example, [1], [3], [13]–[16], and [18] and references therein), and, only recently, reduced-order models utilizable for benchmarking or even for on-line computation (see, for example, [4], [7], and [21]).

An obstacle to the synthesis of dynamic control-oriented models is the description of the chemical phenomena occurring inside the TWC which should be sufficiently flexible to match the behavior of a *large variety* of catalyst formulations and washcoats. Most models employ simplified reaction schemes

and empirical rate expressions, of Langmuir–Hinshelwood type [6], [23], [25], [26], where reaction rates depend on concentrations and temperature at the catalytic sites *along* the reactor.

Unfortunately, the lack of precise kinetic measurements, in particular, during the transient warm-up phase, makes the choice of the suitable expressions and the *tuning* of their parameters probably the most crucial aspects for model reliability. Thus, there is a need for a method allowing the estimation of the kinetic parameters from more easily available experimental data, like temperature and pollutant concentrations profiles at the inlet and the outlet of the converter. In this paper, we present the use of a machine learning technique to solve this problem.

Recently, multilayer neural networks (NN's) have been used for modeling static nonlinear maps with satisfactory results, and novel interconnections of NN's have been tested within dynamic contexts, namely, for the identification of unknown dynamical systems described by a set of ordinary differential equations [24], or as a part of a lumped parameter model [17], [19]. The training is realized through standard gradient methods, such as backpropagation.

Here, we present a novel approach that considers the NN as a subsystem in a partial differential equations (PDE's) model and uses a genetic algorithm (GA) to train it. More precisely, the NN submodel computes the reaction rates of the catalyst during warm-up and is embedded into the TWC PDE's model. This modeling technique allows one to preserve the most important features of an accurate distributed parameter TWC model, it circumvents both the structural and the parameter uncertainty of "classical" reaction kinetics models, and saves computational time. The "*ad hoc*" GA bypasses the above-mentioned problems with the data and the difficulties in applying gradient-based methods in this complex modeling scheme.

This identification procedure requires very short simulation times, achieved here by a purposely designed PDE integration algorithm exploiting the two-time-scale separation of the TWC system.

II. DYNAMIC MODEL OF TWC DURING THE WARM-UP PHASE

In this section, we present the dynamic TWC model described in detail in [7] and [21], which constitutes the backbone of our work. It has been obtained by assuming that the adsorption coefficient between gas and substrate is infinite; this idealization means that, at low temperatures, the adsorption phenomenon is infinitely faster than the chemical reactions taking place on the substrate, and is a reasonable simplification during the warm-up phase [10]. The same can be deduced if one assumes reactions to occur only on the external surface of the catalytic surface [1], [5]. It is a monodimensional PDE's model where the nonuniform flow distribution at the monolith face is neglected
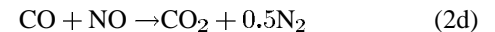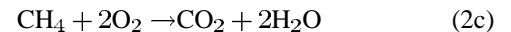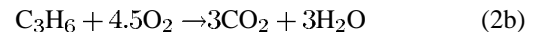
$$v_m(t, x)\rho_g(t, x)c_g\frac{\partial T_g}{\partial x} + hG_A(T_g - T_s) = 0 \quad (1a)$$

$$(1 - \epsilon)\rho_s c_s\frac{\partial T_s}{\partial t} = (1 - \epsilon)\lambda_s\frac{\partial^2 T_s}{\partial x^2} + hG_A(T_g - T_s)$$
$$- h_{\text{amb}}S_{\text{ext}}(T_s - T_{\text{amb}}) - \Delta H^T R'(X, T_s) \quad (1b)$$

$$(1 - \epsilon)\frac{\partial X}{\partial t} = -v_m(t, x)\frac{\partial X}{\partial x} - R(X, T_s). \quad (1c)$$

We consider p chemical species participating in q catalytic reactions and the above equations describe the energy and the mass equilibrium. Pedices "g" and "s" stand for gas and substrate (the reactive surface); T is temperature; X is the p vector of species concentrations expressed in mol/m^3 units and assumed equal in the gas and solid phase in view of the infinite-adsorption hypothesis (see [7] for more details); R is the p vector of specific reaction rates for the species; and R' is the q vector of specific reaction rates for the chemical reactions, both depending on substrate temperature and concentrations; ΔH^T is the q-vector of the heat produced by the catalytic reactions; the independent variables t and x are, respectively, the time and the axial position along the monolith; the various other coefficients are illustrated in the Appendix.

The *minimal* number of reactions significant for the main pollutant considered, e.g., CO, HC and NO, includes six chemical species (CO, C$_3$H$_6$, CH$_4$, H$_2$, O$_2$, NO, hence, $p = 6$; propylene, C$_3$H$_6$, and methane, CH$_4$ summarize many different HC species present in the feedgas). They take part in five chemical reactions ($q = 5$) that describe oxidation of the carbon monoxide CO and unburned hydrocarbons HC, oxidation–reduction of the couple CO–NO and combustion of H$_2$ [3]

$$CO + 0.5O_2 \rightarrow CO_2 \quad (2a)$$
$$C_3H_6 + 4.5O_2 \rightarrow 3CO_2 + 3H_2O \quad (2b)$$
$$CH_4 + 2O_2 \rightarrow CO_2 + 2H_2O \quad (2c)$$
$$CO + NO \rightarrow CO_2 + 0.5N_2 \quad (2d)$$
$$H_2 + 0.5O_2 \rightarrow H_2O. \quad (2e)$$

The reaction with CO is considered as the main path for NO reduction, although other reducing species, such as hydrogen or hydrocarbons, may also contribute to NO conversion.

The structure of the system (1) (see Fig. 2) can be interpreted as the coupling of a thermal subsystem and a chemical subsystem [respectively, (1a) and (1b), and (1c)].

The boundary and initial conditions are ($t \geq 0$, $x \in [0, L]$)

$$\frac{\partial T_s}{\partial t}(t, L) = 0 \quad \text{(Adiabatic constraint)} \quad (3a)$$
$$T_g(t, 0) = T_g^*(t) \quad (3b)$$
$$X(t, 0) = X_g^*(t) \quad (3c)$$
$$T_s(0, x) = T_s^*(x) \quad (3d)$$
$$X(0, x) = X^*(x) \quad (3e)$$

where $T_g^*(t)$ and $X_g^*(t) = (X_{g,1}^*(t), \cdots, X_{g,6}^*(t))^T$ are, respectively, the temperature of the exhaust gas and the concentrations of the chemical species at the inlet of the TWC, $T_s^*(x)$ is the initial temperature of the substrate, $X^*(x) = (X_1^*(x), \cdots, X_6^*(x))^T$ are the initial concentrations, and L is the TWC length.

III. MODELING BY MACHINE LEARNING

A. *The NN for the Reaction Kinetics*

In order to describe the reaction rates employed in model (1), we use the following structure (see Fig. 3):

$$R' = \begin{cases} DR_{NN}(T_s - T_t), & \text{for } T_s \geq T_t \\ 0, & \text{for } T_s < T_t \end{cases} \quad (4)$$
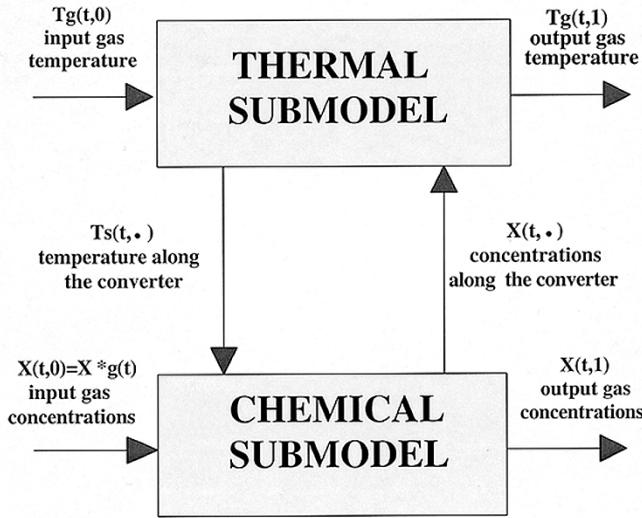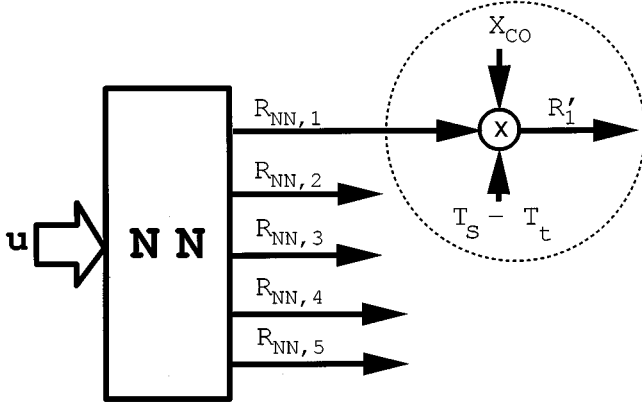
Fig. 2.   Structure of the system.

Fig. 3.   A model of reaction kinetics.

where $R' = (R'_1, \cdots, R'_5)^T$ is the specific reaction rates vector [used in (1b)]; $\boldsymbol{D} \triangleq \mathrm{diag}(X_{\mathrm{CO}}, X_{\mathrm{C_3H_6}}, X_{\mathrm{CH_4}}, X_{\mathrm{NO}}, X_{\mathrm{H_2}}) \in \mathbb{R}^{5 \times 5}$; $R_{NN} \in \mathbb{R}^5$ is the output vector of a fully connected multilayer feedforward NN; T_s is the temperature of the reactive surface (substrate); and T_t is a prefixed temperature threshold. Notice the structure (4) ensures that the kinetic rates are zero in the absence of reactants or when the substrate is at ambient temperature. On the basis of the reaction kinetics it is straightforward to obtain the vector of the rates of the chemical species $R = (R_1, \cdots, R_6)^T$ [(1c)] since it is linearly related to R'

The mathematical model of the NN (see Fig. 4) is completely defined by the number of layers, the specification of the activation function for the neurons in each layer, and the weight matrices for each layer. The NN size has to be chosen according to the tradeoff between model accuracy and computational burden. In our case, a two-layer feedforward neural network is used in the kinetic model and it can be specified as follows:

$$z = \tanh(W_1 u + b_1) \tag{5a}$$
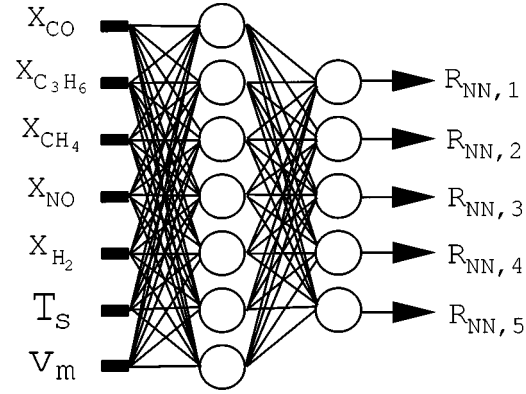$$R_{NN} = W_2 z + b_2 \tag{5b}$$

Fig. 4.   Two-layers network architecture.

where $z \in \mathbb{R}^7$ is the output vector of the first layer; $W_1 \in \mathbb{R}^{7 \times 7}$ and $W_2 \in \mathbb{R}^{5 \times 7}$ are the network weight matrices; $b_1 \in \mathbb{R}^7$ and $b_2 \in \mathbb{R}^5$ are bias column vectors; the $\tanh(\cdot)$ operator is intended component-wise and u is the input vector of the neural net defined as $u = (X_{\mathrm{CO}}, X_{\mathrm{C_3H_6}}, X_{\mathrm{CH_4}}, X_{\mathrm{NO}}, X_{\mathrm{H_2}}, T_s, v_m)^T$. The mean gas velocity in monolith v_m is included in the input vector u because previous identification experiments with the system have shown that this further piece of information improves the performance of the whole model.

B. The Identification Procedure

Since the kinetic data, i.e., inputs and outputs of the net, are not directly available, we have to base the training on the TWC inlet–outlet concentration and temperature profiles. Toward this goal, we use a novel self-organizing GA which solves the following global optimization problem:

$$\min_{W, b} \sum_{h=1}^{7} \frac{1}{v_h} \int_{t_{\mathrm{in}}}^{t_{\mathrm{fin}}} (y_h - \hat{y}_h)^2 \, dt \tag{6}$$

where y is the measured output, $\hat{y}$ is the simulation result, h refers to the output channel of the TWC (temperature and concentrations of the chemical species), v_h are scaling factors, and t_{in} and t_{fin} are, respectively, the initial and final time instants of the simulation.

As is well known, a GA [9] is a stochastic numerical optimization procedure which operates on a *population* of parameter vectors (in this framework, NN parameters). Three "operators" are used to modify the population members:

- *recombination/crossover* which generates new trial solution points (offspring), combining some elements drawn from the population;
- *mutation* which randomly changes some of the offspring components;
- *selection* which chooses the population elements that will be used by the next crossover.

For each population element, a *fitness* is defined, measuring in a quantitative way how the element ranks in the population with respect to the optimization problem. Based on their fitness, the old population members are compared with the newly generated ones, and the solutions with the best fitness constitute the new

population members. In this way, iterating the crossover–mutation–selection process, the population evolves to the optimal solution. Our GA is described in the following.

1) A Self-Organizing GA: This is a real coded GA (i.e., data are not coded as binary numbers as in some schemes) obtained by a modification of the Controlled Random Search (CRS) algorithm by Price [20]. A particular mutation operator, which varies according to the local fitness value and the global success history of the population, allows jumping out of local minima.

Let $G(\lambda)$ be the objective function to be minimized (coinciding here with the fitness function). In a first phase $S > n$ population points are initially randomly chosen according to a uniform distribution within a defined search volume of dimension n. Afterwards, the algorithm, characterized by four parameters (α, β, γ, and G_T) and two variables (I and G_{av}), described later, proceeds as follows.

Step 1) Compute the grid point $\lambda_{\max}$ in which G reaches the maximum value $G_{\max}$, i.e., $G_{\max} = G(\lambda_{\max}) = \max_{i=1,\ldots,S}\{G(\lambda_i)\}$.

Step 2) Form the so-called breeding set, i.e., $n+1$ grid points chosen randomly $\lambda_1, \ldots, \lambda_{n+1}$ (for ease of notation we assume, after renumbering, they are the first $n+1$ population points). All the subsequent operations are performed on this set.

Step 3) *Mutation*: For all the breeding set points λ_i such that $G(\lambda_i) > G_T$, with probability

$$(1 - \alpha^I) \cdot (1 - \beta^{((G(\lambda_i) - G_T)/G_{av})}) \cdot \gamma \qquad (7)$$

replace the point λ_i with a completely random one, chosen within the search volume limits.

Step 4) Iterate Steps 4a and 4b on the whole breeding set.

Step 4a) *Recombination*: For each breeding point λ_i, determine the centroid $\underline{\lambda}_i$ of the other n points, i.e.,

$$\underline{\lambda}_i = \frac{1}{n} \sum_{j=1, j \neq i}^{n+1} \lambda_j. \qquad (8)$$

- Generate the offspring $\lambda_{si} = 2\underline{\lambda}_i - \lambda_i$ (in this way, $\underline{\lambda}_i$ is the midpoint between λ_i and λ_{si}); if λ_{si} is not contained in the search volume, process the next point in the breeding set.
- Compute $G(\lambda_{si})$; if $G(\lambda_{si}) < G_{\max}$, then $\lambda_{\max}$ is purged from the population, and is substituted by the offspring λ_{si}.

Step 4b) *Selection*: Compute the new $G_{\max}$, if necessary.

Step 5) *Convergence test*: $G(\lambda_i) < G_T$ for all $i \in 1, \cdots, S$. If the convergence test is not satisfied, return to Step 1).

The variable I is the number of consecutive iterations in which the population did not change, i.e., no offspring substituted some population member. It gives an empirical measure of the necessity of introducing some fresh information in the population and increases the mutation probability. The variable

G_{av} is the average value of the population fitness, used as a scaling factor.

The parameter G_T is a threshold value used for the convergence test: if all the fitness values of the population are smaller than G_T, the convergence is declared. With this convergence criterion the population points will be clustered inside the domain $\{\lambda: G(\lambda) < G_T\}$. This final cluster can provide useful information about correlations among the unknown parameters as well as information regarding the sensitivity of the cost function to these parameters.

The parameter $\alpha \in [0, 1]$ modulates the mutation rate during the course of the optimization process, and $\gamma \in [0, 1]$ enforces an upper bound to the mutation probability. The term containing the parameter $\beta \in [0, 1]$ provides an ordering of the population members. Namely, members that are farther from convergence, i.e., whose fitness is larger than G_T, have a greater mutation probability. The parameters (α, β, γ) are inherent to the present optimization scheme and may be viewed as modeling coefficients aiding the algorithm to identify its environment; a good choice can increase the rate of convergence of the scheme.

To give an idea of how the recombination mechanism works, Fig. 5 shows two possible grids of six points in a two-parameters space and the offspring obtainable with all possible breeding sets. Notice how the offspring distribution depends on the population shape, in turn determined by the objective function shape, thus exploiting any function regularity. A graphical illustration demonstrating the recombination/mutation mechanism is Fig. 6.

In order to highlight the GA clustering feature, we report its behavior with the Rosenbrock function as a fitness function. The function and limits for the GA are the following:

$$R(x, y) = 74 + 100 \cdot (y - x^2)^2 + (1 - x)^2,$$
$$x, y \in [-2, 2]. \qquad (9)$$

The function $R(x, y)$ has the global minimum in $(1, 1)$, with a quite large banana-shaped basin $R(1, 1) = 74$. We searched for the basin $\{(x, y): R(x, y) \leq 74.2\}$, i.e., $G_T = 74.2$. A population size of 50 elements was used, and the parameters $(\alpha, \beta, \gamma) = (0.25, 0.25, 0.01)$. In Fig. 7 the contour plot of the test function is reported, together with the population in three different stages of the minimization. Convergence has been attained after 500 iterations.

IV. A FAST INTEGRATION ALGORITHM FOR THE PDE MODEL

The TWC reduced model [(1) and (4)] is a distributed parameter model and its simulation times would be prohibitive without using special care in the design of the integration algorithm. We based our algorithm on the fact that: 1) the working of a TWC derives from the interplay of thermal phenomena (thermal exchanges between gas and substrate and thermal energy generated by chemical reactions) and chemical reactions on the substrate [see (1) and Fig. 2] and 2) the thermal phenomena are much slower than the chemical phenomena. Consider now that, when dealing with two-time-scale lumped parameter systems, described via singularly perturbed ordinary differential equations (ODE's) (e.g., [12]), one computes the "slow" subsystem by replacing the fast dynamics with algebraic relations. Here,
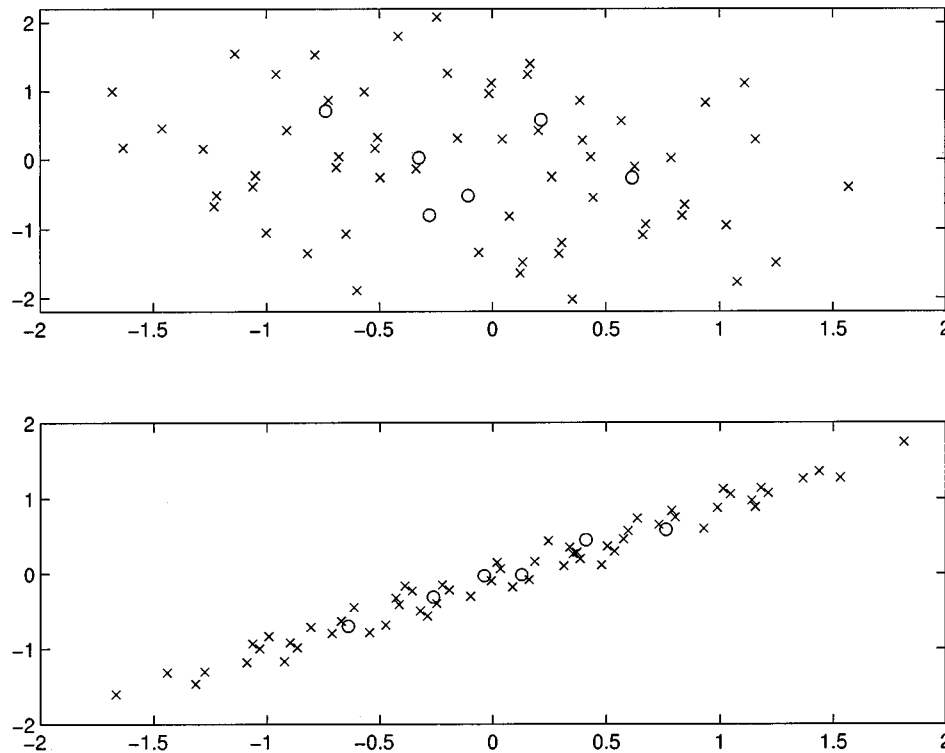
Fig. 5.   Example of the recombination process [formula (8)]. All the possible offspring (crosses) obtainable from two different grid points distributions (circles) (top) uniform grid points distribution; (bottom) clustered grid.
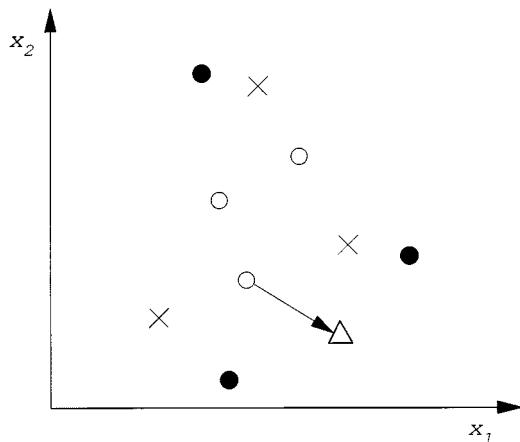

Fig. 6.   Illustration of the mutation/recombination mechanism, for a 2-D parameter space. Circles: original breeding set; crosses: corresponding offspring; triangle: mutated point; bullets: offspring after the mutation.

similarly, we suggest replacing the chemical part of the equation with simple algebraic relations which summarize the conversion efficiencies of the TWC ($\eta_i(t, x)$ for $i = $ CO, $\cdots$, NO); on the other side, since these efficiencies depend on the temperature, their values have to been modified from time to time by integrating the appropriate chemical equations (see Fig. 8).

In particular, taking into account the thermal dynamics, described by (1a), (1b), and the much faster chemical dynamics (1c), we designed the approximate integration scheme that al-

lows the decoupling of the integration procedure as follows (further mathematical details are in [8]).

- Equations (1a) and (1b) have been solved using a finite difference scheme ("method of lines") [22]. The distributed parameter model is converted into a lumped one by a finite difference scheme, thus considering a discrete number of spatial elements, each described by time-varying variables.
- Using the "method of characteristics," the problem of solving the "quasi-linear" hyperbolic PDE's [(1c) with a time-fixed temperature pattern] of the chemical submodel reduces to that of solving a system of ODE's [11].

V. COMPARISON BETWEEN SIMULATION AND EXPERIMENTAL DATA

A. The Experimental Setup

Fully legislated tests have been designed in the U.S. and European Union (UE), respectively, Federal Test Procedure (FPT) cycle and European Control Emissions (ECE) cycle [2], in order to determine whether or not a vehicle meets emissions requirements. The vehicle under test is placed on a chassis dynamometer and driven through the cycle which includes idle drive, accelerations, and decelerations at various rates, and cruises (see, for example, Fig. 9). The tailpipe emissions are collected into bags during the test; the mass of each emission component is then measured and divided by the length of the test to obtain pollutant emissions expressed in grams per mile or kilometer.
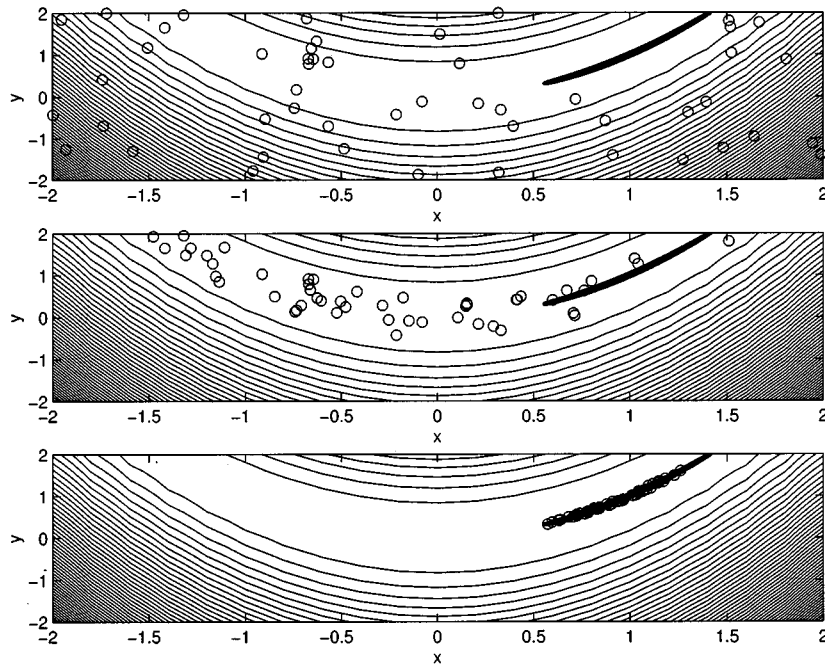
Fig. 7. Thin lines: contour plot of the Rosenbrock function in the search volume limits; black area: target basin; circles: GA population members. From top to bottom: initial population, population after 100 iterations, and final population.
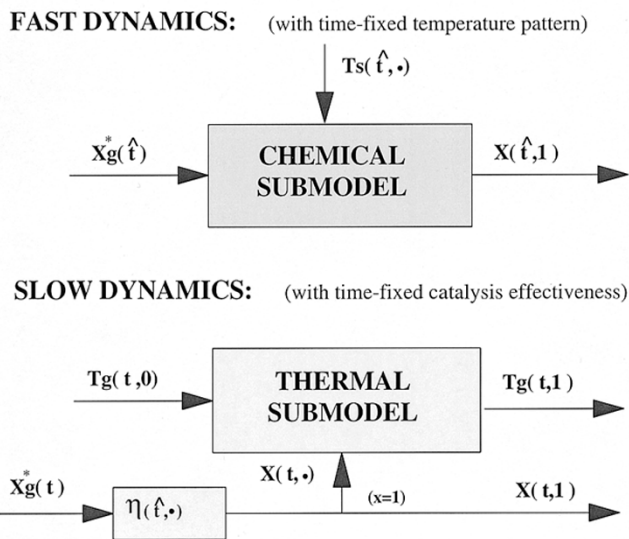
Fig. 8. Approximate system in the time interval $[\hat{t},\ \hat{t} + \Delta t]$.

Fig. 9. ECE cycle—Detail of the "warm-up phase."

Fig. 10. Measurement setup.

For the purpose of building a model of TWC dynamic behavior the experimental data have to provide the *time history* of pre- and post-converter gas temperature and pollutant concentrations in the exhaust gas. Toward this goal, Magneti Marelli Engine Control Division (Bologna, Italy) provided the experimental data. Measurements were conducted on a dynamic test bench consisting of a four-stroke four-cylinder 1400cc FIAT engine equipped with "fresh" (not aged) Pt/Rh converter monolith, a dc motor/generator, and a computerized control facility for all engine input signals. Fig. 10 illustrates the measurement setup.

The input data acquisition rate is 100 Hz. Pollutant measures use three kinds of analyzers: a two-channel flame ion-
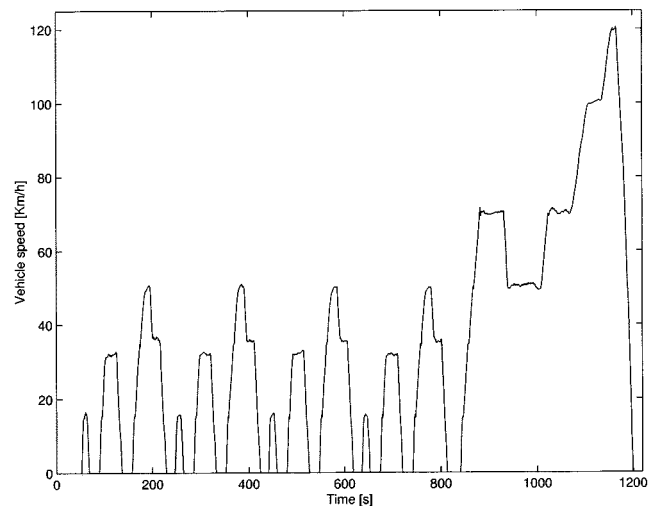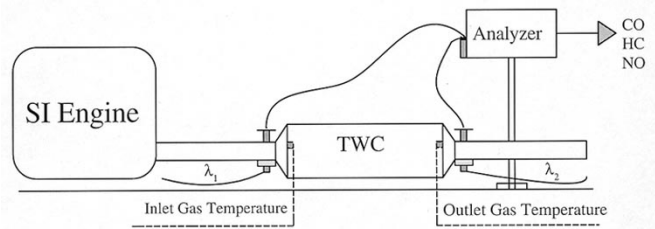
ization detector for HC measurements (time response 0.5 s); a chemi-luminescence analyzer for NO (time response 0.5 s); and a nondispersive infrared detector for CO and CO_2 (time re-
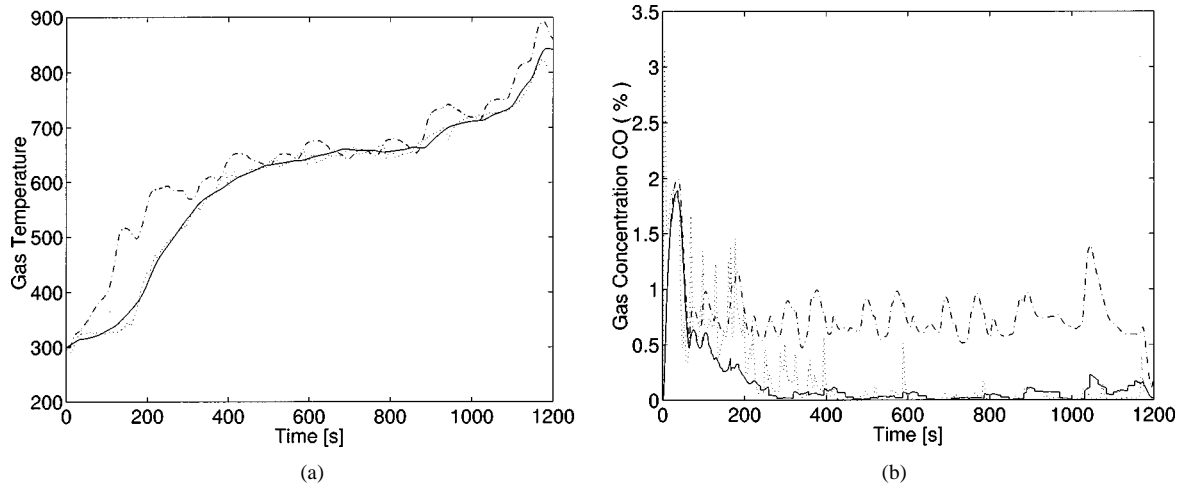
Fig. 11.   (a) T_g time history. (b) CO time history. Dotted line: experimental data referred to the TWC outlet; solid line: model output referred to the TWC outlet; dashed-dotted line: experimental data at the TWC inlet.

Fig. 12.   (a) C_3H_6 time history. (b) CH_4 time history. Dotted line: experimental data referred to the TWC outlet; solid line: model output referred to the TWC outlet; dashed-dotted line: experimental data at the TWC inlet.
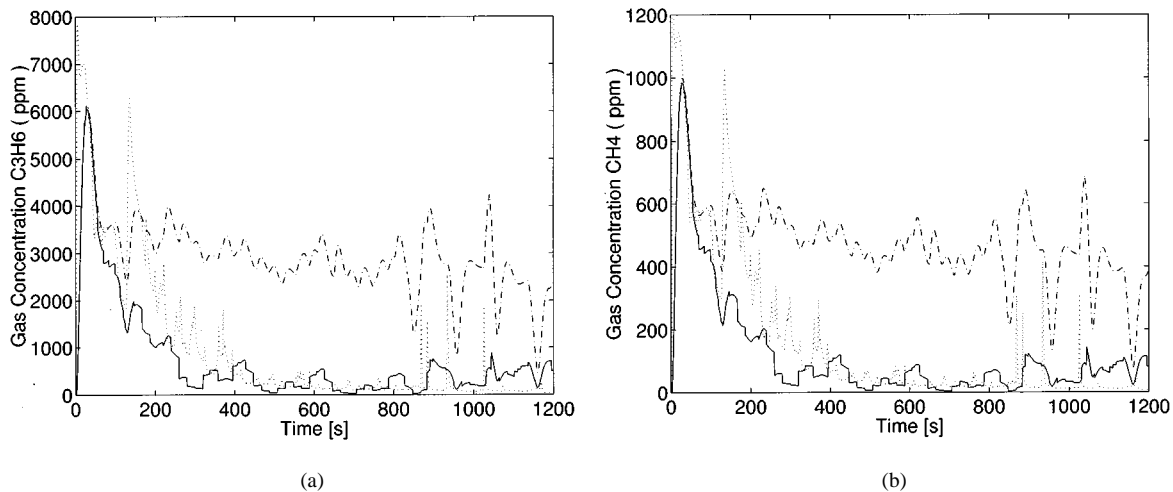
sponse 0.8 s). Thermocouple sensors measure the gas temperature at the inlet and the outlet of the TWC. Pre- and post-catalyst air–fuel ratio is measured with linear exhaust gas oxygen (EGO) sensors (λ_1, λ_2 in Fig. 10) previously heated. The mean exhaust gas velocity is computed from mass air flow (MAF) sensor data. The time delay of the overall acquisition system is about 1.5 s.

B. Results and Discussion

The model behavior is compared to experimental data along the transient thermal phase of an ECE cycle. The simulation of 1200 real seconds of the warm-up along an ECE cycle takes a mere 5 s on a PC, Intel Pentium II 350MHz Processor, 96-Mb RAM; this duration is at least two orders of magnitude smaller than the one obtainable with more standard integration algorithms and "classical" nonlinear kinetic expressions. Our algorithms have been developed on the Matlab 5.2/Simulink 2.0 environment with the support of C-compiled S function.

Simulation results are shown in Figs. 11–13. In all these figures, real TWC input and output data and simulations output are plotted. The parameter identification phase covers the first

800 s of the ECE cycle; the remaining part, which is also rich of dynamics, as one can see in Fig. 9, is used for validation. The model captures the most important features of the TWC warm-up; in particular, the thermal behavior is very well reproduced. As regards the concentrations, the model clearly detects when, due to the low temperature, the catalyst is not properly working. Once the device is sufficiently warm, the conversion is reproduced reasonably well.

Upon closer look, one can notice a mismatch between some peaks of the measurements and the corresponding ones of the model. We point out, however, that the aim of this model is not to describe accurately the catalyst behavior at each time instant, but rather to give a prediction, useful for validation and benchmarking of control strategies, of the main TWC dynamics with very short simulations. From this viewpoint, the approximation obtained has been considered sufficient, even though we plan to collect more startup data (cold start and warm-up) in the future so as to refine the modeling and validation work.

It may be interesting to look at one of the signals R_{NN} multiplied by $T_s - T_t$ (see Fig. 3) because it gives an idea of how the
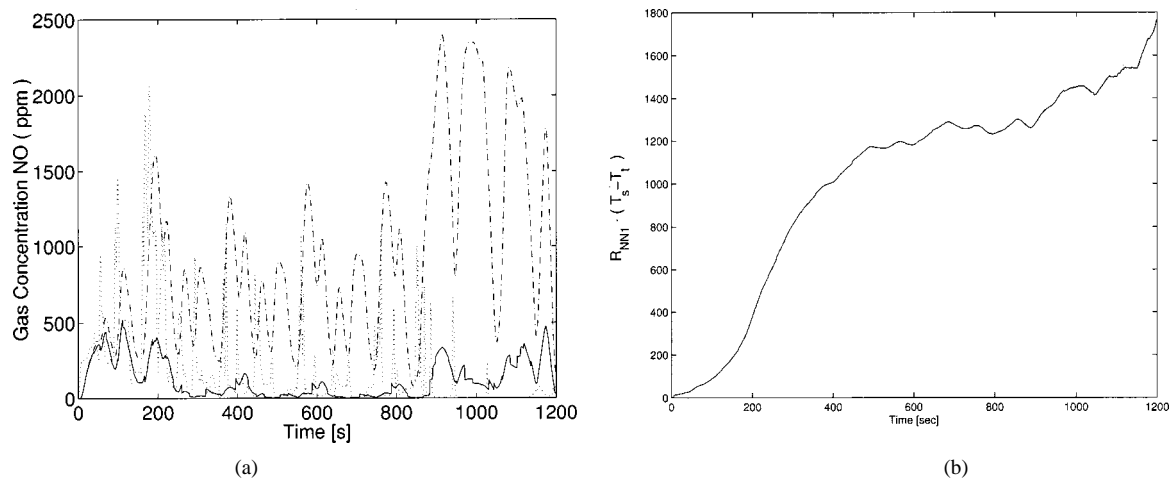
(a)

(b)

Fig. 13. (a) NO time history. Dotted line: experimental data referred to the TWC outlet; solid line: model output referred to the TWC outlet; dashed-dotted line: experimental data at the TWC inlet. (b) Reaction (2a), $R_{NN,1}(T_s - T_t) = R_1'/X_{CO}$ computed at the converter outlet during the TWC warm-up.
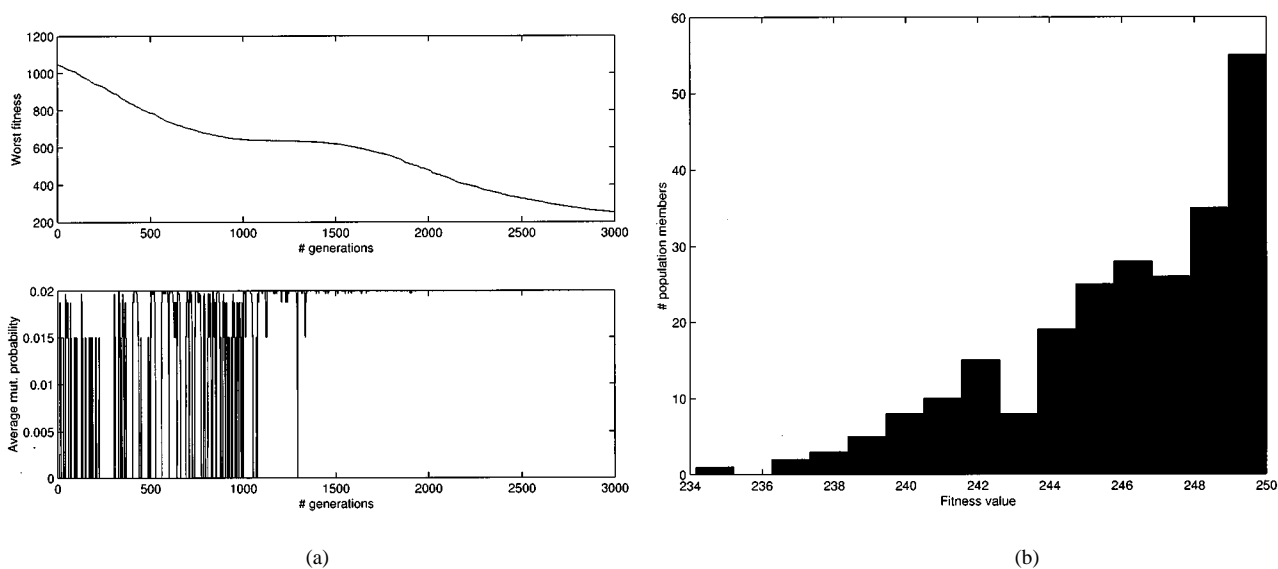

(a)

(b)

Fig. 14. (a) History of worst fitness and mutation probability along generations. (b) Hystogram of fitness distribution among the final population members.

TABLE I
SUMMARY OF THE IDENTIFICATION PROCEDURE

	Two-layer NN
NN structure	$7 \cdot 7 \cdot 5$
Number of parameters	96
Number of population elements	180
(α, β, γ)	$(0.25, 0.25, 0.02)$
Number of generations	3000
Best fitness in last generation	234
Worst fitness in last generation	250

reaction rates R' change during the warm-up phase [Fig. 13(b)]; the scales on the vertical axis do not have a physical meaning since simulations employ an adimensional model.

The identification procedure of the NN submodel is summarized in Table I. Finally, Fig. 14(a) (top) shows how the worst value of fitness in the population decreases along the generations; in Fig. 14(a) (bottom), one can also notice how the mutation probability saturates at its maximum value 0.02 as the

algorithm keeps trying to improve the fitness. The hystogram of Fig. 14(b) illustrates the distribution of the fitness among the final population members.

VI. CONCLUSIONS

The modeling of chemical kinetics is crucial for the modeling of the TWC, but it is very difficult. To bypass this problem, we introduced in this paper a hybrid modeling technique: an NN machine mimics the reaction kinetics inside a PDE model. Furthermore, to overcome the identification obstacles arising from both the lack of direct kinetic data and the whole model structure, we designed a GA for the net training. We showed the validity of this technique using a static two-layer feedforward NN and a fast two-time-scale integration algorithm. We believe that this hybrid approach can be successfully applied to modeling and identification contexts different from ours.

APPENDIX

c_g	J/kg K	specific heat capacity of gas;
c_s	J/kg K	specific heat capacity of substrate;
R_i	mol/m^2·s	specific reaction rate for species i;
R'_l	mol/m^2·s	specific reaction rate for the chemical reaction l;
G_A	m^2/m^3	active area/volume ratio of the monolith;
h	W/m^2 K	convective heat transfer coefficient (from gas to substrate);
h_{amb}	W/m^2 K	heat transfer coefficient;
$k_{D,i}$	m/s	mass transfer coefficient for species i;
S_{ext}	m^2/m^3	external area/volume ratio;
T_{amb}	K	ambient temperature;
v_m	m/s	mean gas velocity in monolith;
ΔH_i	J/mol	heat of ith reaction;
ϵ		void fraction;
ρ_g	kg/m^3	gas density;
ρ_s	kg/m^3	substrate density;
λ_s	W/m K	substrate thermal conductivity (from substrate to ambient);
X_i	mol/m^3	concentration of ith species.

ACKNOWLEDGMENT

REFERENCES

[1] F. Aimard, S. Li, and M. Sorine, "Mathematical modeling of automotive three-way catalytic converters with oxygen storage capacity," *Contr. Eng. Practice*, vol. 4, no. 8, pp. 1119–1124, 1996.

[2] *Automotive Handbook*, 4th ed., R. Bosch GmbH, Stuttgart, Germany, 1996.

[3] N. Baba, K. Ohsawa, and S. Sugiura, "Numerical approach for improving the conversion characteristics of exhaust catalysts under warming-up condition," presented at the SAE Int. Fall Fuels and lubricants Meeting and Exposition, San Antonio, TX, Oct. 1996, SAE Paper 962076.

[4] E. P. Brandt, J. W. Grizzle, and Y. Wang, "A simplified three-way catalyst model for use in on-board SI engine control and diagnostics," in *Proc. ASME Dynamic System and Control Division*, vol. 61, 1997, pp. 653–659.

[5] C. Cussenot, M. Basseville, and F. Aimard, "Monitoring the vehicle emission system components," in *Proc. 13th IFAC World Congr.*, San Francisco, CA, 1996, pp. 111–116.

[6] C. Dubien and D. Schweich, "Three-way catalytic converter modeling. Numerical determination of kinetic data," *Catal. Automotive Pollution Contr. IV—Stud. Surface Sci. Catal.*, vol. 116, pp. 399–408, 1998.

[7] L. Glielmo, S. Santini, and G. Serra, "A two-time-scale infinite-adsorption model of three way catalytic converters," in *Proc. American Control Conf.*, San Diego, CA, 1999, pp. 2683–2687.

[8] L. Glielmo and S. Santini, "A fast integration algorithm for three-way catalytic converters PDE model," in *Proc. 3rd IMACS Symp. Mathematical Modeling*, Vienna, Austria, 2000, pp. 335–338.

[9] D. E. Goldberg, *Genetic Algorithms in Search, Optimization, and Machine Learning*. Reading, MA: Addison-Wesley, 1989.

[10] R. D. Hawthorn, "Afterburner catalysis—Effect of heat and mass transfer between gas and catalyst surface," *AIChE Symp. Ser.*, vol. 70, no. 137, pp. 428–438, 1974.

[11] A. Jeffrey, *Quasilinear Hyperbolic Systems and Waves*. London, U.K.: Pitman, 1976.

[12] P. V. Kokotović, H. K. Khalil, and J. O'Reilly, *Singular Perturbation Methods in Control: Analysis and Design*. London, U.K.: Academic, 1986.

[13] G. C. Koltsakis, P. A. Kostantinidis, and A. M. Stamatelos, "Development and application range of mathematical models for 3-way catalytic converters," *Appl. Catalysis B: Environmental*, vol. 12, no. 2-3, pp. 161–191, June 1997.

[14] G. C. Koltsakis, I. P. Kandylas, and A. M. Stamatelos, "Three-way catalytic converter modeling and applications," *Chem. Eng. Commun.*, vol. 164, pp. 153–189, 1998.

[15] E. Leveroni, K. N. Pattas, A. M. Stamatelos, P. K. Pistikopoulos, G. C. Koltsakis, P. A. Konstandinidis, and E. Volpi, "Transient modeling of 3-way catalytic converters," presented at the SAE Int. Conf. and Exposition, Detroit, MI, Feb. 28–Mar. 3, 1994, SAE Paper 940934.

[16] C. Montreuil, S. C. Williams, and A. A. Adamczyk, "Modeling current generation catalytic converters: Laboratory experiments and kinetic parameter optimization—Steady state kinetics," , Detroit, MI, Feb. 1992, SAE Paper 920096.

[17] K. Narendra and K. Parthasarathy, "Identification and Control of Dynamic Systems using Neural Networks," *IEEE Trans. Neural Networks*, vol. 1, pp. 4–27, Mar. 1990.

[18] S. H. Oh and J. C. Cavendish, "Mathematical modeling of catalytic converter lightoff. Part III: Prediction of vehicle exhaust emissions and parametric analysis," *AIChE J.*, vol. 31, no. 6, pp. 943–949, June 1985.

[19] I. H. J. Ploemen and M. J. G. van de Molengraft, "Hybrid modeling for mechanical systems: Methodologies and applications," *J. Dynam. Syst., Meas., Contr.*, vol. 121, no. 2, pp. 270–277, 1999.

[20] W. L. Price, "A controlled random search procedure for global optimization," *Comput. J.*, vol. 20, no. 4, pp. 367–370, 1976.

[21] S. Santini, "Some innovative modeling, identification and control techniques for automotive applications," Ph.D. dissertation, Dip. Inform. Sistem., Univ. Studi Napoli Federico II, Naples, Italy, Nov. 1999.

[22] W. E. Schiesser, *The Numerical Method of Lines: Integration of Partial Differential Equations*. San Diego, CA: Academic, 1991.

[23] B. Subramanian and A. Varma, "Reaction kinetics on a commercial three-way catalyst: The carbon monoxide–nitrogen monoxide–oxygen–water system," *Ind. Eng. Chem. Product Res. Develop.*, vol. 24, no. 4, pp. 512–516, 1985.

[24] W. Wang and C. Lin, "Runge–Kutta neural networks for identification of dynamical systems in high accuracy," *IEEE Trans. Neural Networks*, vol. 9, pp. 294–307, Mar. 1998.

[25] S. E. Voltz, C. R. Morgan, D. Liederman, and S. M. Jacobs, "Kinetic study of carbon monoxide and propylene oxidation on platinum catalysts," *Ind. Eng. Chem. Product Res. Develop.*, vol. 10, no. 3, pp. 294–301, 1973.

[26] ——, "Kinetic study of carbon monoxide and propilene oxidation on platinum catalysts," *Ind. Eng. Chem. Product Res. Develop.*, vol. 12, no. 4, pp. 202–209, 1994.

Luigi Glielmo (S'84–A'85–M'90) received the "Laurea" degree in electronic engineering and the Research Doctorate degree in automatic control from the Università di Napoli Federico II, Naples, Italy, in 1986 and 1990, respectively.

He is currently an Associate Professor of Automatic Control in the Department of Computer and System Engineering, Università di Napoli Federico II. His theoretical research interests include analysis and robust control design through Lyapunov and singular perturbation techniques, and extended Kalman filtering. On the application side, he has worked on ship dynamic positioning, and plasma shape identification and control for Tokamak fusion reactors. Since 1995, he has been involved in automotive control, particularly, reduced-order modeling of three-way catalytic converters, idle speed and A/F control, supervision control for vehicle subsystems integration, dry clutch control, and hybrid vehicle simulation. He is an Associate Editor of *Dynamics and Control*.

Prof. Glielmo is currently the Chairman of the Technical Committee on Automotive Controls of the IEEE Control Systems Society. He is a member of the Society for Industrial and Applied Mathematics, ASME, and Society of Automotive Engineers.

Michele Milano was born in Naples, Italy, in 1969. He graduated in electronic engineering from the Università di Napoli Federico II, Naples, Italy, in 1996. He is currently working toward the Ph.D. degree at the Institute of Fluid Dynamics, Swiss Federal Institute of Technology, Zürich, Switzerland.

During 1997, he was at the Swiss Federal Institute of Technology as an Academic Guest, working on the application of neurocomputing techniques to the control of combustion engines. His Ph.D. thesis work, developed in collaboration with the NASA Center for Turbulence Research, Moffett Field, CA, deals with the application of machine learning techniques to flow modeling and control. His research interests include neural networks, fuzzy logic, genetic algorithms, and control systems.

Stefania Santini graduated in electronic engineering and received the Ph.D. degree in automatic control (supported by the Italian National Research Council Engine Institute) from the Università di Napoli Federico II, Naples, Italy, in 1996 and 1999, respectively.

During 1998, she was with the Laboratory of Engine Systems, Swiss Federal Institute of Technology, Zürich, Switzerland, as an Academic Guest, working on modeling, simulation, and identification of internal combustion engines. She is currently a Post-Doctoral Researcher in the Department of Computer and System Engineering, Università di Napoli Federico II. Her primary research interests are automotive control, particularly, modeling and control of exhaust after-treatment systems, A/F and idle speed control, and hybrid electric vehicle simulation and control.